

## Coplanar Ternary Cluster Decay of Hyper-deformed $^{56}\text{Ni}$

G. Efimov, V. Zhrebchevsky, W. von Oertzen, B. Gebauer, S. Thummerer,  
Tz. Kokalova, Ch. Schulz, H.G. Bohlen, D. Kamanin, C. Beck, et al.

► **To cite this version:**

G. Efimov, V. Zhrebchevsky, W. von Oertzen, B. Gebauer, S. Thummerer, et al.. Coplanar Ternary Cluster Decay of Hyper-deformed  $^{56}\text{Ni}$ . 2007. in2p3-00169805

**HAL Id: in2p3-00169805**

**<http://hal.in2p3.fr/in2p3-00169805>**

Preprint submitted on 5 Sep 2007

**HAL** is a multi-disciplinary open access archive for the deposit and dissemination of scientific research documents, whether they are published or not. The documents may come from teaching and research institutions in France or abroad, or from public or private research centers.

L'archive ouverte pluridisciplinaire **HAL**, est destinée au dépôt et à la diffusion de documents scientifiques de niveau recherche, publiés ou non, émanant des établissements d'enseignement et de recherche français ou étrangers, des laboratoires publics ou privés.

# Coplanar Ternary Cluster Decay of Hyper-deformed $^{56}\text{Ni}$ .

G. Efimov<sup>a,d</sup> V. Zhrebchevsky<sup>a,f</sup> W. von Oertzen<sup>a</sup>  
B. Gebauer<sup>a</sup> S. Thummerer<sup>a</sup> Tz. Kokalova<sup>a</sup> Ch. Schulz<sup>a</sup>  
H. G. Bohlen<sup>a</sup> D. Kamanin<sup>a,d</sup> C. Beck<sup>b</sup> D. Curien<sup>b</sup>  
M. Rousseau<sup>b</sup> P. Papka<sup>b</sup> G. Royer<sup>c</sup> G. de Angelis<sup>e</sup>

<sup>a</sup>*Hahn-Meitner-Institut-GmbH, Berlin, Germany*

<sup>b</sup>*IPHC, Département de Recherches Subatomiques, IN2P3-CNRS UMR7178  
Université Louis Pasteur, Strasbourg, France*

<sup>c</sup>*Subatech, UMR: Université-IN2P3/CNRS-Ecole des Mines, Nantes, France*

<sup>d</sup>*Flerov laboratory for Nuclear Reactions, JNR, Dubna, Russia*

<sup>e</sup>*Laboratori Nazionali di Legnaro, Legnaro, Italy*

<sup>f</sup>*St. Petersburg University, St. Petersburg, Russia*

---

## Abstract

Coincidences between two heavy fragments have been measured from fission of  $^{56}\text{Ni}$  compound nuclei, formed in the  $^{32}\text{S} + ^{24}\text{Mg}$  reaction at  $E_{lab}(^{32}\text{S}) = 163.5$  MeV. A unique experimental set-up consisting of two large area position sensitive (x,y) gas-detector telescopes has been used allowing the complete determination of the observed fragments, and their momentum vectors. In addition to binary fission events with subsequent particle evaporation, narrow out-of-plane correlations are observed for two fragments emitted in purely binary events and in events with a missing mass consisting of  $2\alpha$  and  $3\alpha$ -particles ( $^{12}\text{C}$ ). These events are interpreted as ternary cluster decay from  $^{56}\text{Ni}$ -nuclei at high angular momenta through hyper-deformed shapes.

*Key words:* NUCLEAR REACTIONS,  $^{24}\text{Mg} + ^{32}\text{S}$ ,  $E_{lab} = 163.5$  MeV; Kinematic coincidences for heavy fragments, out-of-plane correlations, binary and ternary fission channels

*PACS:* 25.70.Jj, 25.70.Pq, 24.60.Dr

---

## 1 Introduction

Clustering and large deformations are observed as general phenomena at low excitation energy in light  $N=Z$  nuclei. Super- and hyper-deformed shapes are predicted at higher excitation energies and at high angular momenta in nuclei with masses ranging from  $A = 20$  up to 100, see [1–6]. For these nuclear configurations shell corrections for quadrupole deformation parameters  $\beta_2=0.6-1.0$ , corresponding to major-to-minor axis ratios of 2:1 up to 3:1 (for ellipsoidal shapes) play an important role. These states are typically found at energies, which are several MeV lower than the liquid drop values. The deformed shell corrections will stabilise the rotating nucleus in its super- and hyper-deformed shapes at lower angular momentum [5] and in some cases enhanced  $\gamma$ -transitions can be expected to be observed over several spin values. In the present work the cluster decay of the hyper-deformed states is considered.

Configurations showing the cluster structure of the hyper-deformed states in  $^{56}\text{Ni}$  were obtained with the Brink-Bloch  $\alpha$ -cluster model [2], highlighting the relation between large deformations and clustering. This work suggests that hyper-deformed states in  $^{56}\text{Ni}$  will fission into several clusters, in particular at high angular momentum. Furthermore, ternary fission is predicted for such nuclei using an approach based on the generalised liquid drop model [7,8], taking into account the proximity energy and quasi-molecular shapes as obtained in the  $\alpha$ -cluster model [2]. The ternary cluster decay has in the present mass range a less favourable Q-value as compared to the binary mass split, however, particular mass splits are predicted to be favoured [2] also from SU(3) cluster-structure considerations [9]. As will be shown in the following, however, ternary cluster decay can be strongly enhanced for the largest deformations due to the lowering of the fission barrier obtained with the large moments of inertia and by the afore mentioned shell corrections. Until now experimental evidence for such ternary break-up has only been reported [10,11] by our group for  $^{60}\text{Zn}$  with the similar experimental set-up. Searches for hyper-deformation in heavier nuclei via  $\gamma$ -decay at high angular momentum [12] have shown that its identification is a very difficult task, because the probability of the fission decay will be increased.

We have studied fission events from the decay of the  $^{56}\text{Ni}$  compound nucleus (CN) at an excitation energy of  $E_{CN}^* = 83.8$  MeV, formed in the  $^{32}\text{S}+^{24}\text{Mg}$  reaction at  $E_{lab} = 163.5$  MeV. The incident energy was chosen to correspond to the  $E_{CN}^*$  of the last broad resonance [13] observed in the  $^{28}\text{Si}+^{28}\text{Si}$  channel. In the experiment two heavy fragments are measured in coincidence. The compound nucleus decay in the  $^{32}\text{S}+^{24}\text{Mg}$  system has been studied extensively by Sanders et al. [14]. From this pioneering work some basic information on the CN formation is available. For instance, the maximum angular momen-

tum reached for  $^{56}\text{Ni}$ , is close to  $45\hbar$ , consistent with the predicted liquid-drop limit [15]. At these high angular momenta the binary fission decay can reach up to 10% of the total fusion cross section, which leads dominantly to evaporation residues. In the present work ternary fission is identified by the coincident registration of two fragments with a measured total charge much lower than the compound nucleus. This is done with a unique experimental set up, which allows the full coverage of the in-plane and out-of-plane angular correlations. The ternary fission decay in the present case competes at high angular momentum with the binary fission due to the formation of hyper-deformed configurations.

## 2 Experimental conditions

The experiment was performed at the VIVITRON Tandem facility of IReS (Strasbourg) with the BRS-EUROBALL set-up [16,17,20] aimed at particle- $\gamma$ -spectroscopy. Two detector telescopes, labelled 3 and 4, are located symmetrically on either side of the beam axis. Each of them comprise two-dimensional position-sensitive low-pressure multi-wire chambers (MWC) and Bragg-curve ionisation chambers. In the reaction, schematically written as:

$(M_1, Z_1) + (M_2, Z_2) \rightarrow ^{56}\text{Ni}^* \rightarrow (M_3, Z_3) + (\Delta Z) + (M_4, Z_4)$ , two heavy fragments with masses  $(M_3, M_4)$  and charges  $(Z_3, Z_4)$  are registered in kinematical coincidence and identified by their charges. The masses could not be fully determined in this experiment, details of the detectors and the experimental set-up are given in [21].

With the position sensitive detectors the correlations have been measured between two heavy ejectiles for in-plane and out-of-plane scattering angles,  $\theta$  and  $\phi$ , respectively. Other parameters measured are the Bragg-peak height  $BP$ , the range  $R$  and the rest energy  $E$ , giving the identification of the fragments by their charge and momentum vectors. A typical two-dimensional spectrum of  $BP$  versus  $E$  is shown in Fig. 1. The two detectors cover in-plane angles, of  $\theta_L = 12.5^\circ - 45.5^\circ$ , and in their centre planes the out-of-plane angles  $\phi$  ranges are  $\Delta\phi = 0^\circ \pm 16.8^\circ$ , or  $180^\circ \pm 16.8^\circ$ . The centre of mass angular ranges are with the “inverse” kinematics in the region  $\theta_{cm} = 70^\circ - 125^\circ$ . The relation  $(\phi_3 - \phi_4) = 180^\circ$  for the out-of-plane angles defines coplanarity condition, the reaction plane is defined by the beam axis and the two vectors of the emitted heavy fragments.

The  $^{24}\text{Mg}$  targets consisted of  $240 \mu\text{gr}/\text{cm}^2$  enriched to 99.9% on a layer of  $20 \mu\text{gr}/\text{cm}^2$  of  $^{12}\text{C}$ . For the later discussion the potential contributions from oxygen on the target are of importance. Further the  $^{12}\text{C}$ -backing can influence the systematics of the yields based on the spectra of two fragments with charges  $(\Delta Z = 6)$  in coincidence. Reaction channels are defined by the the

sum of the observed charges of the fragments, ( $Z_{CN} = Z_3 + Z_4 + \Delta Z$ ), with different values of  $\Delta Z = 0 - 8$ . This procedure gives information for channels with a well defined missing charge  $\Delta Z = (Z_{CN} - Z_3 - Z_4)$ .

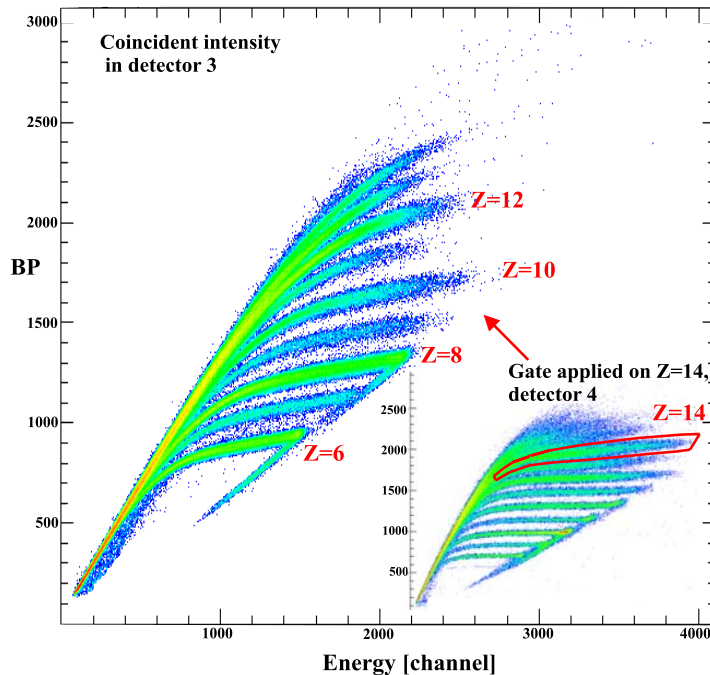


Fig. 1. Bragg-peak-Energy distributions of events in detector 3 obtained in coincidence with a  $Z = 14$  gate in detector 4 as shown in the insert for the reaction  $^{32}\text{S} + ^{24}\text{Mg} \rightarrow Z_3 + Z_4 + \Delta Z$ .

For binary exit-channels, with two heavy fragments which do not evaporate particles, very narrow out-of-plane  $\phi$ -distributions must be observed. For non-binary channels broad distributions (broad in the  $\phi$ -distributions) appear, because of the missing information on the momenta of the unobserved third particles.

For the following discussion of ternary events these out-of-plane correlations are essential. The fragment yields,  $N(Z_3, Z_4)$ , are plotted in Fig. 2 as function of  $(\phi_3 - \phi_4)$  for some combinations of  $Z_3$  and  $Z_4$ , with *even total charge*, but different  $\Delta Z$ . The coplanarity condition is fulfilled for purely binary events ( $Z_3 + Z_4 = 28$ ) in the form of a narrow peak around  $(\phi_3 - \phi_4) = 180^\circ$ . The small broader component in the out-of-plane angular correlations is the result from neutron evaporation. No narrow correlation is observed for  $\Delta Z = 2$  (first column in Fig. 2), where the corresponding recoil of the evaporated  $\alpha$ -particles widens the angular correlation. These events correspond to binary fission with an excitation energy being sufficiently high for one  $\alpha$ -particle to be evaporated from either of the fission fragments.

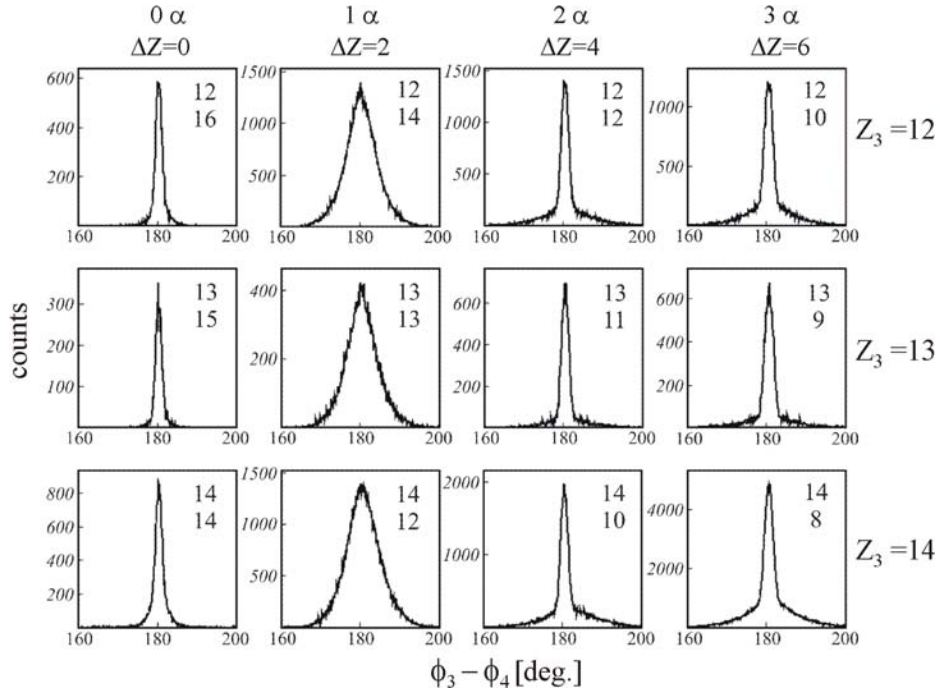


Fig. 2. Yields (counts),  $N(Z_3, Z_4)$  for  $(Z_3 + Z_4) = \text{even}$ , of coincident fragments with charges  $Z_3$  and  $Z_4$ , as indicated, as a function of the out-of-plane angles  $(\phi_3 - \phi_4)$ , in degrees. The out-of-plane angular correlations show differing width for binary decay (col.1) and for the respective non-binary emission channels with missing  $\Delta Z = 1\alpha$ (col.2),  $2\alpha$ (col.3), and  $3\alpha$ (col.4) in the reaction  $^{32}\text{S} + ^{24}\text{Mg}$  at  $E_{lab} = 163.5$  MeV.

The expectation is that for larger charge losses  $\Delta Z > 2$  (a sequential emission of several charged particles) the  $\phi$ -correlations will have increasing width (see [10,11]). This is fulfilled with a broader component, e.g. for two missing  $\alpha$ -particles,  $\Delta Z = 4$  (col.3), and for  $\Delta Z = 6$  (col.4) in Fig. 2. For  $\Delta Z = 4$  and 6 small broad components are observed. A non-negligible contribution from reactions on  $^{16}\text{O}$  in the target is present in the narrow part of  $\Delta Z = 4$  and in the broad part for  $\Delta Z = 6$ . The narrow component in  $\Delta Z = 4, 6$  remains comparable (factor 2) to the yield of the purely binary case, except for the channels with  $(Z=8, ^{16}\text{O})$ . As we will see later, the narrow parts, after subtraction of the  $^{16}\text{O}$  contribution can be described (as in ref. [10]) by coplanar ternary cluster decay.

Whereas the purely binary decay has a small yield, the yields corresponding to the emission of  $1\alpha$ -particle are the largest at this incident energy (see also [10,21]), and are broad in the  $\phi$ -correlations due to the momentum spread induced by the recoil in the evaporation process. The yields in these broad distributions are typically 5-8 times stronger than the for purely binary channel. This fact gives us the possibility to estimate the contributions from the potential target contaminants, for the reaction on  $^{16}\text{O}$ : e.g.  $^{32}\text{S} + ^{16}\text{O} \rightarrow ^{28}\text{Si} + ^{20}\text{Ne}$  (corresponding to  $\Delta Z = 4$  from the target  $^{24}\text{Mg}$ ). The narrow compo-

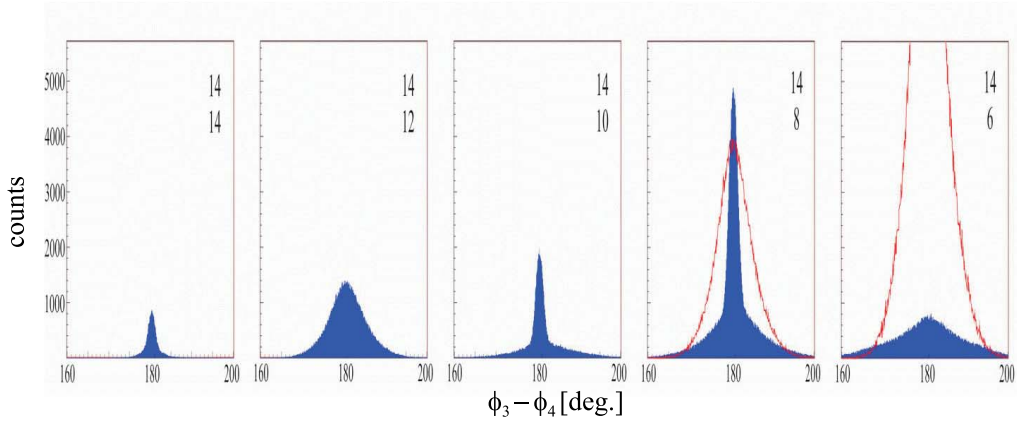


Fig. 3. Out-of-plane angular correlations  $N(\phi_3 - \phi_4)$  with a fixed gate on  $Z_4$  for binary coincidences (compare with Fig. 2) and the respective emission channels with missing  $\Delta Z = (1-4)\alpha$ . The expected broad yield in  $\Delta Z = 6, 8$  are shown for the assumption that the narrow components in  $\Delta Z = 4, 6$  are fully due to the contaminants  $^{16}\text{O}$  and  $^{12}\text{C}$ , respectively.

nents from  $^{12}\text{C}$  in the target, e.g. reaction  $^{32}\text{S} + ^{12}\text{C} \rightarrow ^{28}\text{Si} + ^{16}\text{O}$  corresponds to  $\Delta Z = 6$  relative to the target  $^{24}\text{Mg}$ . If all events in the narrow components in the  $\Delta Z = 4$  would originate from a binary process on  $^{16}\text{O}$ , a corresponding strong wide component from the reaction  $^{32}\text{S} + ^{16}\text{O} \rightarrow ^{28}\text{Si} + ^{16}\text{O} + 1\alpha$  (about factor 5) must appear in  $\Delta Z = 6$  (see Fig. 3, thin (red) line distribution). However, the broad component in  $\Delta Z = 6$  is smaller than expected, the event rate is a factor 3 to small (see also the same procedure in ref. [10]). Similarly, if we assume that the observed narrow  $\Delta Z = 6$  component originates from  $^{12}\text{C}$  alone, the expected yield of the  $(-1\alpha)$ -broad component in  $\Delta Z = 8$  should be 4 times larger. Actually for  $^{12}\text{C}$ , the kinematic conditions for the sum energies and angles are unfavourable in the regions of  $\theta_L = 12.5^\circ - 45.5^\circ$  spanned by the BRS, thus binary reactions on  $^{12}\text{C}$  can only give small contributions. These observations show that the narrow distributions in the yields  $N(\phi_3, \phi_4)$  are only partially due to the reactions on the  $^{24}\text{Mg}$  target. The determination of the amount of contributions from contaminants is discussed below.

For the further discussion of the contaminants we investigate the correlation with *odd total charges* (see Fig. 4). No very narrow peaks appear in  $\Delta Z = 1$ , because of the emission of a proton. The increase of the width from  $\Delta Z = 1$  to  $\Delta Z = 3$  is clearly due to the (additional) emission of the  $\alpha$ -particle. For  $\Delta Z = 5$ , however, we observe again a narrower peak as observed in  $\Delta Z = 1$ . The Q-value for the loss of  $2\alpha$ -particles and 1proton for the  $^{24}\text{Mg}$ -target is very negative, so that this contribution to  $\Delta Z = 5$  is very small. We can safely assume that the third column in Fig. 4 corresponds completely (almost 100%) to the reaction with  $\Delta Z = 1$  on the  $^{16}\text{O}$  in the target, which has a less negative Q-value. From this realistic assumption, we can determine the  $^{16}\text{O}$ -content by assuming that the fission into fragments with  $(-1p)$ -evaporation on both  $^{16}\text{O}$

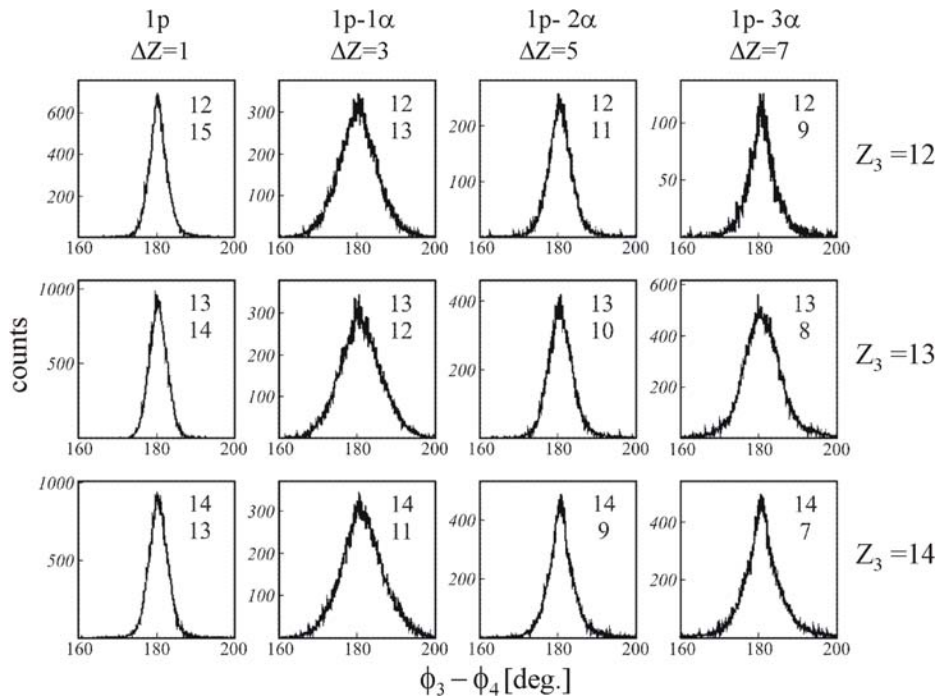


Fig. 4. Yields,  $N(Z_3, Z_4)$  for  $(Z_3 + Z_4) = \text{odd}$ , as a function of  $(\phi_3 - \phi_4)$ , in degrees (out-of-plane angular correlations) for coincident fragments with charges as indicated.

and on  $^{24}\text{Mg}$  have the same cross section (in the cm-system). This procedure gives a 45 %  $^{16}\text{O}$ -content in the  $^{24}\text{Mg}$ -target of  $240 \mu\text{g}/\text{cm}^2$ .

### 3 Reaction mechanisms

As an overview on the reaction mechanism giving the narrow components in the  $\phi$ -correlations, we can consider three different mechanisms.

i) Pre-fission emission of  $\alpha$ -particles: fission of the CN after the emission of nucleons or of one or two (and even more)  $\alpha$ -particles. Such pre-scission process will not disturb the correlation of the two remaining fission fragments. We can rule out this process, because a second chance fission [14,23] after particle emission is very unlikely. From the systematics of Morgenstern [24] the average energy carried by one nucleon is 16.4 MeV and by one  $\alpha$ -particle is 23.4 MeV. In the pre-equilibrium emission of one nucleon or  $\alpha$ -particle this amount of energy or more must be removed. Furthermore, no significant contribution from a narrow peak in the  $\phi$ -correlations is observed for the fragment-fragment coincidences with one missing charge or for  $\Delta Z = 2$ .

ii) A strong spin alignment of the binary fission fragments: e.g. for  $\Delta Z = 4$  (with sequential emissions) with their angular momenta completely aligned perpendicular to the reaction plane. The alignment from the first step has to



be preserved for the whole set of data. The fact that narrow  $\phi$ -correlations still appear for  $\Delta Z= 4, 6$  makes it rather unlikely that such a special correlation is created and persists through all decays.

iii) Ternary fission: the missing  $\alpha$ -particles have only a small momentum perpendicular to the reaction plane. A prompt (simultaneous) ternary decay with the  $\alpha$ -particles in the neck is unlikely, rather we must consider two subsequent fission processes in a time sequence with two neck ruptures in a short time interval. In this case the emission of the third fragment in the second step would occur in the reaction plane [11].

If the third clustered fragments are preformed in the neck of the composite nucleus the two remaining heavier fragments are emitted in a sharp correlation as in the case of a purely binary fission process. As explained below, due to the energy balance the ternary process can only occur for the highest angular momenta, and the decay has to be collinear, therefore the value of  $(\phi_3 - \phi_4)$  remains  $180^\circ$ . We note that in an earlier measurement, performed with the BRS-spectrometer for the reaction  $^{36}\text{Ar} + ^{24}\text{Mg}(\text{CN} - ^{60}\text{Zn})$  at  $E_{lab} = 195$  MeV, under similar conditions the same unique narrow correlations with  $(\phi_3 - \phi_4) = 180^\circ$  have been observed [10,21].

The definition of reaction channels is obtained by the choice of the sum  $(Z_3 + Z_4)$  and the broad or narrow part of the  $\phi$ -correlations. The corresponding differential cross sections are shown in Fig. 5, they represent the average value for the angular ranges (centre of mass) of ca  $70^\circ$ - $125^\circ$ . The angular distribution in the mentioned range are flat [10,11,18] and are symmetric around  $90^\circ$ . For the broad part, interpreted as binary fission with a corresponding excitation in the fragments for particle evaporation to occur, a subtraction of the  $^{16}\text{O}$ -contribution is made for the  $-3\alpha$ -channel. For the narrow component (ternary fission) in the  $(-2\alpha$  and  $-3\alpha)$ -channels the reduction in both cases by a factor 0.45. The strong odd-even effect in the yields is as expected from statistical-model predictions, which was also discussed in ref. [10,11].

The absolute values of the differential cross sections in the cited channels shown in Fig. 5 are actually very close to those observed in [10,11] for the fission of  $^{60}\text{Zn}$  with similar excitation energy and angular momentum. This agreement between two completely independent experiments is very important. A difference appears for the compound nucleus  $^{56}\text{Ni}$  with the high yield of  $(Z_3 + Z_4 = 14 + 8)$ , which is observed in both the broad (this can not be influenced by  $^{16}\text{O}$ -contributions) and the narrow components. In the statistical model calculations of [22] the yield for this channel is enhanced due to the favourable Q-value, this work also shows the odd-even effect in the yields. The differences in the yields for the different Q-values between the odd and even channels, and the more favourable Q-value (by 5 MeV) of the channels with  $Z = 8$  are consistent with the observed higher yields.

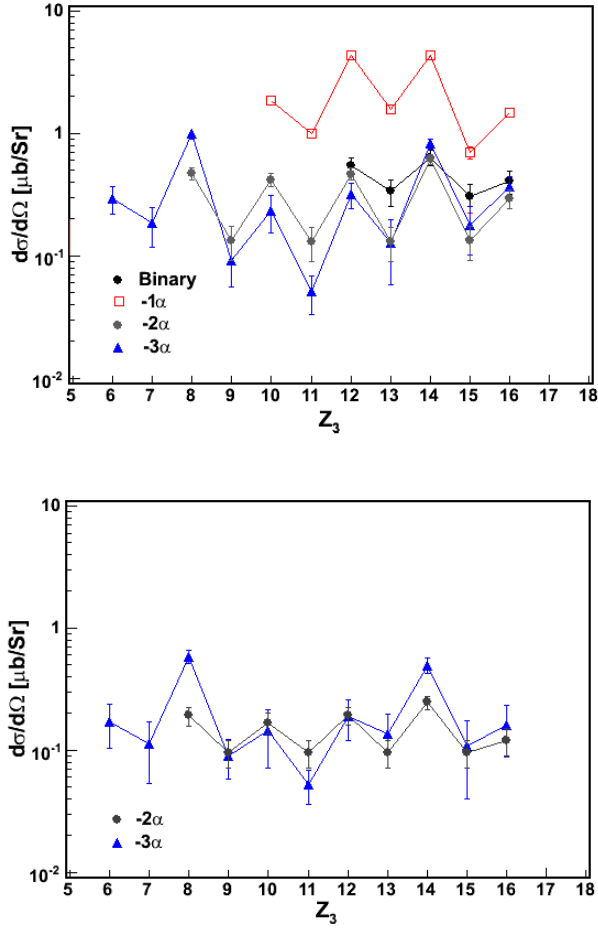


Fig. 5. Yields of binary ( $\Delta Z = 0, 2, 4, 6$ ) and ternary ( $\Delta Z = 4, 6$ , lower part) coincident fission fragments. The respective non binary emission channels are with missing  $\Delta Z = (2)-1\alpha, (4)-2\alpha$ , and  $(6)-3\alpha$ -particles from the reaction  $^{32}\text{S} + ^{24}\text{Mg}$  at  $E_{lab} = 163.5$  MeV (colour online).

The higher yield in the channels with  $Z = 8$  could also be explained by the decay of a hyper-deformed resonant state, which is known at exactly the chosen excitation energy in the  $^{56}\text{Ni}$  nucleus (populated due to the choice of the incident energy on top of a  $^{28}\text{Si} + ^{28}\text{Si}$  resonance), described in [2,27]. The shape as predicted in the cluster model is shown in Fig. 6, the formation of  $^{16}\text{O}$  is favoured for all shapes.

The narrow components in the  $\phi$ -correlations appear at  $(\phi_3 - \phi_4) = 180^\circ$ . For this fact a comment on the geometrical shape of the fission saddle and the three-body configuration is needed. The three fragments could be placed at different relative orientations, however, it can easily be shown that for larger values of the total spin  $J$ , the *collinear configuration*, which has the largest moment on inertia relative to all others, gives the lowest fission barrier. This feature has been calculated for some specific cases by Wiebecke and Zhukov [25]. Thus we indeed expect a collinear decay with  $(\phi_3 - \phi_4) = 180^\circ$ , with the ternary

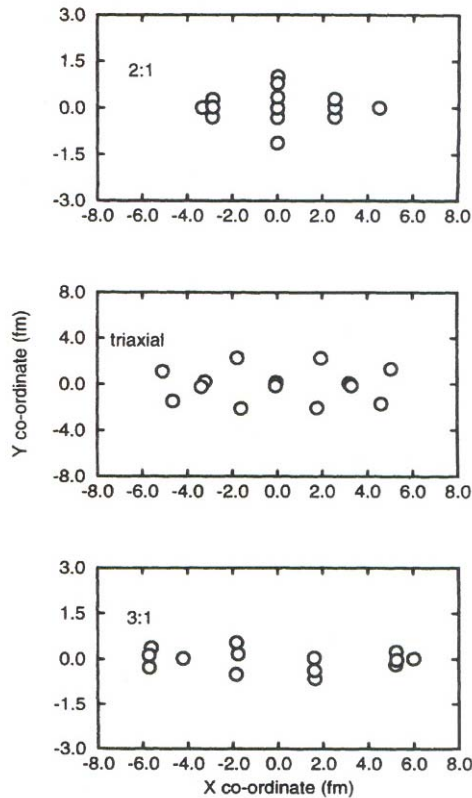


Fig. 6. Clusterisation of the highly deformed  $^{56}\text{Ni}$  nucleus in the Brink-Bloch-Cluster model as obtained by Zhang et al. [2]. Different binary and ternary decay channels with the formation of  $^{28}\text{Si}$ ,  $^{24}\text{Mg}$ ,  $^{16}\text{O}$  and  $^{12}\text{C}$  are expected to be favoured.

fission dominantly occurring at the highest angular momenta. The result also indicates that the missing particles are multiples of  $\alpha$ -clusters. Such behaviour is predicted by the  $\alpha$ -cluster model in [2] for the hyper-deformed shapes of  $^{56}\text{Ni}$  at high angular momentum, which are shown in Fig. 6. From this figure we may also conclude that the triaxial configuration may dominantly decay into  $^{24}\text{Mg} + 2\alpha + ^{24}\text{Mg}$ , whereas the axially symmetric one would decay into  $^{16}\text{O} + 3\alpha + ^{28}\text{Si}$ . Both channels strongly contribute to the ternary fission.

#### 4 Statistical model for fission

A major point in the interpretation of the data is to explain the strong yield of the “ternary” fission channels in view of their more negative Q-values. However, e.g. for the binary decay with  $3\alpha$ -particles emitted the fragments must be excited, the Q-values are thus similar to the ternary decay with  $3\alpha$ -particles missing. For the interpretation of the data as a fission process from an equilibrated CN, we have to consider the statistical phase space for both binary and coplanar ternary fission. This can be achieved by considering the Ex-

tended Hauser-Feshbach Method (EHFM) [23]. For ternary events, implying  $N\alpha$ -particles in the neck, we make the assumption that their momentum in the centre of mass is small. We will disregard the phase space of these particles, as well as their kinetic energy. For a CN with excitation energy,  $E_{CN}^*$ , a ternary Q-value  $Q_{gs}(3, 4)$ , and excitation energies of the fragments given by  $U_3, U_4$ , with their relative kinetic energy as  $E_{kin}(3, 4)$ , we have the constraint for the excitation energies:  $U_3 + U_4 = E_{CN}^* + Q_{gs}(3, 4) - E_{kin}(3, 4)$ . The two excitation energies are connected, both fragments being registered in coincidence before further decay. The excitation energies,  $U_3$  and  $U_4$ , are below the  $\alpha$ -decay threshold, which for even-even nuclei with ( $N=Z$ ) is in the region of 5-8 MeV.

The differential cross section for different mass partitions ( $i, j$ ) depends on the *product of the level densities*  $\rho_i(U_i, J_i), \rho_j(U_j, J_j)$ , for  $i = 3, j = 4$  and on the “inverse fusion” cross section  $\sigma(E_{kin}(3, 4), R_s, J)$

$$\frac{d\sigma(3, 4)}{d\Omega dE_{kin}(3, 4)} = C\rho_3(U_3, J_3)\rho_4(U_4, J_4)\sigma(E_{kin}(3, 4), R_s, J) \quad (1)$$

$J_3$  and  $J_4$  are the spins of the fragments (with total spin  $J$ ), and  $R_s$  distance between fragments for the choice of the configuration ( $R_s = R_3 + R_4 + d$ , where  $d$  is a neck parameter). For the total energy balance, with potential energy  $V_{pot}^{eff}(J, 3, 4, R_s)$ , which includes the rotational energy. We define the free energy which is available for the fragments (to be excited or emitted in their ground states):

$$E_{free}(3, 4, J) = E_{CN}^* + Q(3, 4) + V_{pot}^{eff}(J, 3, 4, R_s) \quad (2)$$

This value will determine the yield for a particular partition. The rotational energy  $E_{rot}(J, 3, 4, R_s)$  depends on the total spin  $J$  and on the moment of inertia  $\Theta_{ff}(R_s)$ . The total potential contains the shell corrections  $\Delta_{sh}(R_s)$  at the deformed saddle point:  $V_{pot}^{eff}(J, 3, 4, R_s) = E_{rot}(J, 3, 4, R_s) + V_{pot}(3, 4, R_s) + \Delta_{sh}(R_s)$ . The values of the shell corrections (in the range of 5-8 MeV) to the saddle point of hyper-deformed shapes are particular large for  $N = Z = 28$ , and can be found in the review of Ragnarson et al. [6].

The interpretation of the relative yields of the binary and ternary fission yields can be obtained from these considerations, they will be determined by:

- a) the Q-values, namely different values of  $E_{free}(3, 4, J)$  (also different values of  $U_i$  and  $U_j$  needed for particle evaporation),
- b) the shell corrections for large deformations (3:1 axis ratio),
- c) the angular momentum. Because of the different moments of inertia  $\Theta_{ff}$ , for binary (normally deformed) and ternary (hyper-deformed) shapes, the corresponding differences in fission barrier heights become smaller at high  $J$  values

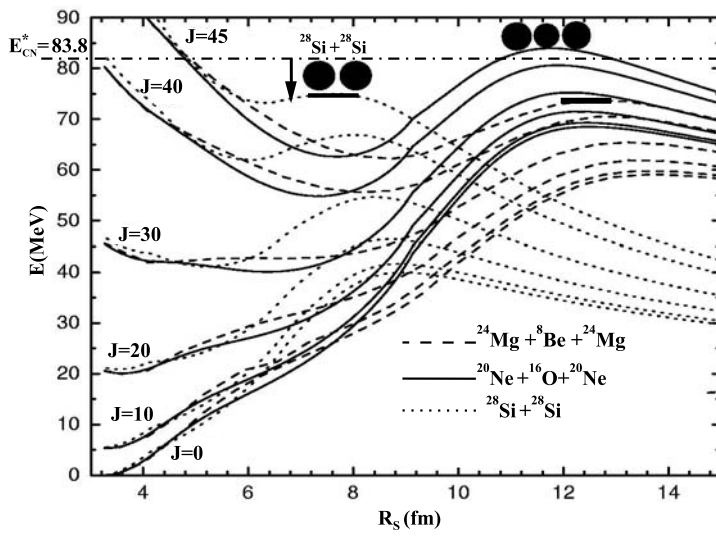


Fig. 7. Potential energies for selected fragmentations in the decay of  $^{56}\text{Ni}$  as a function of the deformation (represented by the distance  $r$  between the two heavier fragments) for different angular momenta (in units of  $\hbar$ ) for binary and ternary fission, respectively. Channels with different  $\Delta Z$ , (missing 2 and  $4\alpha$ -particles) are shown. The barriers and the free energy (indicated by the arrow) are marked. The Q-value for,  $^{28}\text{Si}+^{28}\text{Si}$  is +3.04 MeV, and  $Q = -16.9$  MeV for the ternary decay with  $^8\text{Be}$  ( $-2\alpha$ ).

(see fig. 7). Some relevant values are summarised in Table 1.

Table 1

Q-values, the inverse of the moments of inertia ( $\hbar^2/2\Theta_{ff}$ ) and barrier heights (in MeV) for some fission channels of  $^{56}\text{Ni}$ .

Reactions	$\hbar^2/2\Theta_{ff}$	$Barrier(J = 45)$	Q-value [MeV]
<i>Binary</i> , $-0\alpha$ , $^{28}\text{Si} + ^{28}\text{Si}$	0.038	73.5	+ 3.04
<i>Binary</i> , $-0\alpha$ , $^{20}\text{Ne} + ^{36}\text{Ar}$	0.041	75.7	- 2.67
<i>Binary</i> , $-0\alpha$ , $^{22}\text{Na} + ^{34}\text{Cl}$	0.040	74.7	- 10.3
<i>Ternary</i> , $-2\alpha$ , $^{24}\text{Mg}+^{24}\text{Mg}$	0.015	76.6	- 16.93
<i>Ternary</i> , $-2\alpha$ , $^{26}\text{Al}+^{22}\text{Na}$			- 27.40
<i>Ternary</i> , $-2\alpha$ , $^{28}\text{Si}+^{20}\text{Ne}$			- 16.26
<i>Ternary</i> , $-3\alpha$ , $^{24}\text{Mg}+^{20}\text{Ne}$	0.014	78.9	- 26.24
<i>Ternary</i> , $-3\alpha$ , $^{22}\text{Na}+^{22}\text{Na}$	0.0154	80.9	- 36.86
<i>Ternary</i> , $-3\alpha$ , $^{28}\text{Si}+^{16}\text{O}$			- 20.99
$-1p - 2\alpha, (^{24}\text{Mg}), ^{20}\text{Ne}+^{27}\text{Al}$			- 27.85
$-1p$ , (on $^{16}\text{O}$ ), $^{16}\text{O}+^{31}\text{P}$			- 8.86

In the calculations by Royer [8], the liquid-drop energies, the Q-values and the rotational energies constitute the main part of the barrier heights for the

fission process. With the angular momentum dependence of  $V_{pot}^{eff}(J, 3, 4, R_s)$ , the free energy  $E_{free}(3, 4, J)$  at the saddle point is dramatically reduced (see Fig. 7) for both the binary and the ternary mass splits as a function of  $J$ . The ternary barrier becomes comparable to the binary barrier, and the difference in Q-values being compensated by the smaller value of  $E_{rot}(J, 3, 4, R_s)$ . In Table 1 we show the Q-values and the rotational energies at the saddle point for  $J = 45\hbar$ . The Q-values are more negative for ternary mass splits, therefore negligible contributions are expected at low angular momentum. The ternary fission process from the hyper-deformed configuration is expected to be enhanced due to a lowering of its ternary fission barrier by the shell corrections. The Q-values for the ternary mass splits with odd-odd charge fragments are in addition 5-10 MeV more negative. Thus, in these cases much lower yields and less subsequent decays via particle evaporation are possible.

## 5 Conclusion

We conclude that the observation of the narrow coplanar fission fragment coincidences in the present data, in conjunction with the earlier work on the same phenomenon for  $^{60}\text{Zn}$  in [10,11], is a unique feature, which gives evidence for the occurrence of ternary decay processes in excited  $N=Z$  nuclei. The ternary coplanar fission is a signature of the decay from an extremely deformed nucleus at high angular momentum. Although a detailed analysis within the statistical model still needs to be undertaken, the relative yields in the different channels clearly show the odd-even staggering expected as function of charge, with the lower yields for the negative Q-values in the odd-odd channels. Remarkable is the preference for particular cluster decays, also expected from the statistical phase space, e.g. in the case of  $^{28}\text{Si} + ^{12}\text{C} + ^{16}\text{O}$ . The result indicates that the highly deformed nucleus  $^{56}\text{Ni}$  is clustered, and the formation of a resonance (obtained by the choice of the incident energy) with a particular shape contributes to the observed fission yield systematics. The populated state is well described in the Brink-Bloch cranked  $\alpha$ -cluster model [2], its shape was shown in Fig. 6.

This work also shows that the search for hyper-deformation in rapidly rotating nuclei, can be pursued with charged-particle spectroscopy. The neck represents a region of low nuclear density favouring the formation of  $\alpha$ -clusters as recently discussed by Horiuchi [26]. For nuclei in the medium-mass region a complete reconstruction of the ternary fission events can be undertaken with appropriate detector systems. Thus, measurements of the ternary fission process offer the possibility of detailed spectroscopy of extremely deformed nuclear states.

We would like to acknowledge the help of the EUROBALL-group of IReS during the experiment. We thank the VIVITRON crew for their excellent

support. This work was supported by the ministry of research (BMBF, Germany) under contract Nr.06-OB-900, and by EC-Euroviv contract HPRI-CT-1999-0078. Tz. Kokalova and V. Zhrebchevsky thank the DAAD for their support. We thank C. Wheldon for his numerous helps in this project.

## References

- [1] S. Cohen, F. Plasil and W. J. Swiatecki, *Ann. Phys. (N.Y.)* **82** (1974) 557.
- [2] J. Zhang, A. C. Merchant, and W. D. M. Rae, *Phys. Rev. C* **49** (1994) 562 and W.D.M. Rae in *Proc., 5<sup>th</sup> Intern. Conf. on Clustering Aspects in Nuclear and Subnuclear Systems 1988*, Kyoto, *Prog. Theor. Phys. (Jap.)* ed. K. Ikeda, (1989) p. 80.
- [3] G. Leander and S. E. Larsson, *Nucl. Phys. A* **239** (1975) 93.
- [4] S. Aberg, H. Flocard and W. Nazarewicz, *Ann. Rev. Nucl. Science*, Vol. **40** (1990) 439.
- [5] S. Aberg and L.O. Joensson, *Z. Phys. A* **349** (1994) 205.
- [6] I. Ragnarsson, S. Aberg and R. K. Sheline, *Phys. Scr.* **24**, 215 (1981); I. Ragnarsson, S. G. Nilsson and R. K. Sheline, *Phys. Rep.* **45** (1978) 1.
- [7] G. Royer and F. Haddad, *J. Phys. G* **21** (1995) 339.
- [8] G. Royer, *J. Phys. G* **21** (1995) 249; also G. Royer, F. Haddad and J. Mignen, *J. Phys. G* **18** (1992) 2015.
- [9] A. Algora, J. Cseh et al. *Phys. Lett. B* **639** (2006) 451, and private communication.
- [10] V. I. Zhrebchevsky, W. von Oertzen, et al., *Phys. Lett. B* **646** (2007) 12.
- [11] V. I. Zhrebchevsky, W. von Oertzen, D. V. Kamanin, *JETP Lett.* Vol. 85, N.3, (2007) 136. Also Dr.Thesis, St. Petersburg University, 2007.
- [12] B. Herskind et al., 2003, in “Achievements with the Euroball spectrometer”, eds. W.Korten and S. Lunardi
- [13] R. Betts et al., *Phys. Rev. Letters* **47** (1981) 23.
- [14] S.J. Sanders, A. Szanto de Toledo and C. Beck, *Phys. Rep.* **311** (1999) 487 and references therein.
- [15] C. Beck and A. Szanto de Toledo, *Phys. Rev. C* **53** (1996) 1989.
- [16] B. Gebauer et al., in *Proc. Int. Conf. on the Future of Nucl. Spectroscopy*, Crete, Greece, 1993, eds. W. Gelletly et al., p. 168.
- [17] B. Gebauer et al., *Achievements with the Euroball spectrometer*, 2003, eds. W. Korten and S. Lunardi, p. 135.

- [18] G. Efimov et al., to be published and Dr.Thesis, Dubna University. 2007.
- [19] N. Curtis et al., Phys. Rev. **C 53** (1996) 1963.
- [20] C. Beck et al., Nucl. Phys. **A 734** (2004) 453.
- [21] S. Thummerer et al., Nuovo Cimento **111 A** (1998) 1077.
- [22] A. V. Andreev et al., Eur. Phys. J. **A 30** (2006) 579.
- [23] T. Matsuse, C. Beck, R. Nouicer and D. Mahboub, Phys. Rev. **C 55** (1997) 1380.
- [24] H. Morgenstern et al., Z. Phys. **A 313** (1983) 39.
- [25] H. J. Wiebecke and M. Zhukov, Nucl. Phys. Nucl. Phys. **A 351** (1981) 321.
- [26] H. Horiuchi, Nucl. Phys. **A 731** (2004) 329.
- [27] C. Beck et al., Phys. Rev. **C 63** (2001) 014607.